RSC Advances

ROYAL SOCIETY OF CHEMISTRY

www.rsc.org/advances

Three-dimensional light confinement in PT-symmetric nanocavity

Wenzhao Sun,[a‡] Zhiyuan Gu,[a‡] Shumin Xiao,[b§] and Qinghai Song[a*]

Received Xth XXXXXXXXXX 20XX, Accepted Xth XXXXXXXXX 20XX
First published on the web Xth XXXXXXXXXX 200X
DOI: 10.1039/b000000x

Light confinement and manipulation in nanoscale have gained intensively research attention due to their potential applications ranging from cavity quantum electrodynamics to nano-networks. Within all these researches, the effective mode volume (V_{eff}) is the key parameter that determines the light-matter interaction. While various nanocavities have been developed in past decades, very few has successfully confined light within nanoscale in all three dimensions. Here we demonstrate a robust mechanism that can improve the light confinement in nanostructures. By breaking the parity-time (PT) symmetry in nanowire based nanocavities, we find that the resonant modes are mostly localized at the interfaces between gain and loss regions, providing an additional way to confine light along the third direction. Taking a hybrid plasmonic Fabry-Perot cavity as an example, we show that the V_{eff} has been dramatically improved from $\sim$ 0.0092 μm^3 to $\sim$ 0.00169 μm^3 after the breaking of PT symmetry. In additional to the perfect PT symmetric cavities with ($n(r) = n(-r)^*$), we have also observed similar three-dimensional light confinements and ultrasmall V_{eff} in quasi-PT symmetric systems with fixed losses. We believe that our finding will significantly improve the light-matter interaction in nanostructures and help the advances of their applications.

The rapid developments in nano-networks and nano-devices have triggered intensively research attention in nanoscale coherent light sources [1–3]. In past decade, the sizes of lasers have been quickly reduced from microscale to subwavelength and eventually to nanoscale [4–6]. Several schemes have been utilized to generate nanosized light confinements, e.g., photonic crystal nanocavity [1], nanorods and nanowires [6], and plasmonic nanocavities [4]. Spaser, which is pioneered by Bergman and Stockman [7], is a prominent example. By replacing the photon and resonances with surface plasmon and plasmonic mode, spasers have been successfully observed in a 44-nm-diameter gold-dyed silica core-shell nanoparticle [8]. To date, spasers have been demonstrated in many systems including, nanoantenna [9], nanoparticle arrays [10], and hybrid plasmonic waveguide [11]. Compared with the other spapers or nanolasers, the hybrid plasmonic nanolasers are extremely interesting because they combine the advantages of single crystalline nanowires and surface plasmon polaritons, and they have the potentials to be compatible to conventional CMOS technology.

Soon after the first experimental demonstration [11], hybrid plasmonic lasers have been reported in GaN [12], CdS [13], GaAs [14], and ZnO [15] based nano-systems and the V_{eff} has been dramatically reduced. While the hybrid plasmonic systems can give extremely small effective mode area (on the order of nm^2), the values of V_{eff} are limited by the lengths of nanowires or waveguides. In this sense, hybrid plasmonic waveguides are only nice platforms for two-dimensional light confinements. In the third direction, they mainly function as conventional Fabry-Perot cavities. Although periodic structures such as photonic crystals have been utilized to improve the light confinement in the third direction [16], the designs are usually too complicated for practical applications. Therefore, it is highly desirable to find a simple way to confine light in full three dimensions. Here we explore one possibility by combining the surface mode and two-dimensional light confinement in hybrid plasmonic waveguide. By breaking the parity-time (PT) symmetry in nanolasers, surface modes have been generated at the gain-loss interface. Consequently, a full three-dimensional light confinement has been formed and the V_{eff} has been greatly reduced.

Our finding is based on the recently developed PT symmetry in non-Hermitian system [17]. Due to the generality of gain and loss in optical systems, PT symmetry has been widely studied in past few years [18–20,22–25]. A number of unique properties such as perfect absorbers [19], non-reciprocity [20], unidirectional invisibility [21], and single mode microlasers [22–25] have been designed and experimentally realized. Here we study the PT symmetry within hybrid plasmonic nanolasers. Figure 1(a) depicts the schematic picture of the designed structure. A CdS nanowire with radius R=100 nm and length L=10 μm is placed onto a MgF_2 coated Ag films. The thickness of MgF_2 and Ag films are fixed at 5 nm and 100 nm, respectively. This is one

[a] *Integrated Nanoscience Lab, Department of Electrical and Information Engineering, Harbin Institute of Technology, Shenzhen, China. Fax: 86 755 2603 2022; Tel: 86 755 2661 2207; E-mail: qinghai.song@hitsz.edu.cn*
[b] *Integrated Nanoscience Lab, Department of Electrical and Information Engineering, Harbin Institute of Technology, Shenzhen, China. Fax: 86 755 2603 2022; Tel: 86 755 2661 2207; E-mail: shumin.xiao@hitsz.edu.cn*
‡ These authors contributed equally to this work.§∗ Corresponding to shumin.xiao@hitsz.edu.cn and qinghai.song@hitsz.edu.cn

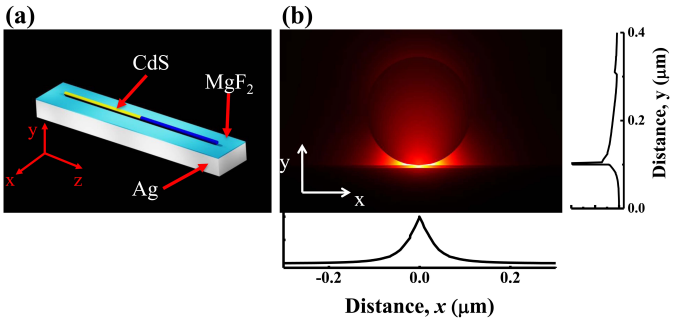

Fig. 1 Schematic picture of the designed nanocavity and the field confinement (a) A CdS nanowire with radius R is placed onto a MgF_2 coated Ag film. The gain and loss are applied in the yellow and blue regions of CdS nanowire. (b) The mode profile in the transverse plane.

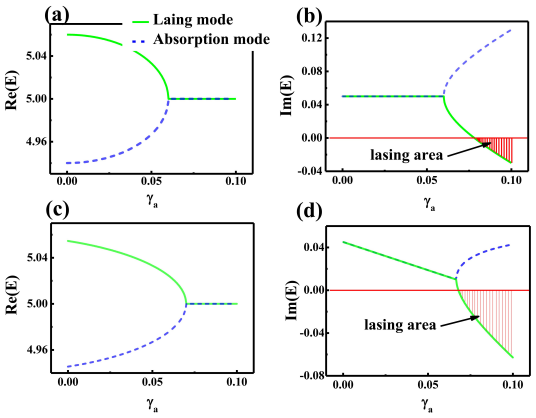

Fig. 2 PT symmetry and quasi-PT symmetry. (a) and (b) are the real and imaginary parts of the eigenfrequencies (E) as a function of γ_a under perfect PT symmetry. (c) and (d) are similar to (a) and (b) except $\gamma_b = -0.05$. The other parameters are $\kappa = 0.05$, $J = 0.06$.

of the typical structures of hybrid plasmonic nanocavity. It can also switch to metal-coated Si waveguide for the top-down fabrication process. In general, plasmonic nanolasers can be generated by pumping the nanowire entirely. Such nanolasers are well confined within the gap region (see Fig. 1(b))[26]. From the transverse field distributions, it is easy to see that the lights are confined within tens of nanometers in both x and y directions.

The situation changes when the gain and loss are introduced to the CdS nanowire. As depicted in Fig. 1(a), the nanowire is subdivided from the center and then gain and loss are applied to the left (yellow) and right (blue) regions in Fig. 1(a). Here the gain and loss are defined with the refractive index as $n_L = n_0 + n_1''i$, and $n_R = n_0 + n_2''i$. For CdS nanowire, n_0 is fixed at 2.55 and the imaginary parts are set as $n_1'' = -n_2''$ to form the PT symmetry. For the case of passive cavity ($n_1'' = n_2'' = 0$), the resonant modes travel individually and do not cross-talk. While the situation is different when the PT-symmetric configuration is applied to the cavity. The two initial resonant modes at resonance frequencies ω_a and ω_b with adjacent mode number supported by the F-P nanocavity have the possibility to couple one another. With the increase of gain and loss, the amplitudes of the two resonances are strongly modified and redistribute. Thus the resonance behaviors of the non-Hermitian system depicted in Fig. 1(a) can be predicted by the coupled-mode theory via the following equations[27]

$$i\frac{da}{dt} = \omega_a a + i(\gamma_a - \kappa)a + Jb, \quad (1)$$

$$i\frac{db}{dt} = \omega_b b + i(\gamma_b - \kappa)b + Ja, \quad (2)$$

where a and b are their respective modal amplitudes, $\gamma_{a,b}$ are their associated gain and loss rates, κ is the intrinsic loss of the metal, J is the real-valued coupling constant. By considering the perfect PT symmetry with $\omega_a + \omega_b = 2\omega_n$, and $\gamma_a = -\gamma_b = \gamma_n$, the eigenfrequencies can be written as

$$\omega_\pm = \omega_n \pm \sqrt{J^2 - \gamma_n^2} - i\kappa, \quad (3)$$

Figures 2(a) and 2(b) have shown the resonant behaviors with perfect PT symmetry with $\gamma_a = -\gamma_b$. When the gain factor γ_a is small, the real parts of two resonances slightly approach one another and the imaginary parts are kept as constant at κ. Once γ_a is larger than the coupling constant J, the real part of frequencies merge to ω_n, whereas the imaginary parts quickly bifurcate[19,28]. One mode becomes more lossy. The other mode reaches the threshold (Im(E) = 0) and becomes a lasing mode. At the point $\gamma_a = J$, both the real parts and imaginary parts of two resonances are the same, clearly showing the well-known exceptional point.

In additional to the perfect PT symmetric system, we have also studied the systems with fixed loss. Compared with perfect PT symmetric systems, this setting is more practical in experiments. This is because that the gain is much easier to be tuned than the loss. It can be simply realized by selectively pumping[29]. But the increase in loss usually relies on the complicated carrier injection or bias voltage. In quasi-PT symmetric systems, the eigenfrequencies E of Eqs. (1) and (2) can be expressed as

$$\omega_\pm = \omega_n \pm \sqrt{J^2 + (\frac{\Delta\omega}{2} + i\frac{\gamma_a - \gamma_b}{2})^2} - i(\frac{\gamma_a + \gamma_b}{2} - \kappa), \quad (4)$$

where $\Delta\omega = \omega_a - \omega_b$ is the detuned condition. Then the resonant behaviors can also be predicted from Eq. (4).The calcualted results are shown in Figs. 2(c) and 2(d). We can see that the basic behaviors are similar to the case of perfect P-T symmetric system. With the increase of γ_a, the real parts

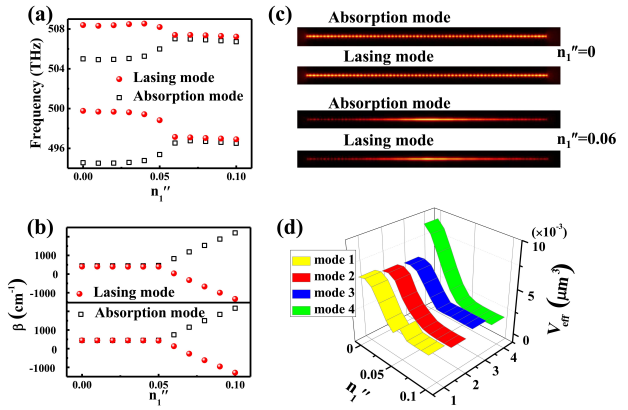

Fig. 3 PT symmetry breaking in hybrid plasmonic nanocavity. (a) and (b) are the dependencies of resonant frequency (Re(f))and β (Im(f/100c)) value on n_1''. (c) The field patterns along x-z plane within MgF_2 gap with n_1'' = 0 (top) and n_1'' = 0.06 (bottom). (d) The V_{eff} as a function of n_1''.

of the eigenfrequencies gradually approach and merge. And their imaginary parts bifurcate after the PT symmetry breaking. The only difference is that the imaginary parts of two modes increase simultaneously before the exceptional point and then bifurcate[27].

Based on above theoretical analysis, we numerically study the structure with commercial finite element method package (COMSOL multiphysics 4.3a). The dielectric constants of MgF_2 is 1.9 and the dispersion of Ag is defined with Drude model. Perfect matched layers have been used to absorb the outgoing waves. Thus the resonances inside hybrid plasmonic structure are quasi-bound modes with complex eigenfrequencies (f). The real part of the frequency (Re(f))corresponds to the resonant wavelength and the imaginary part relates to the loss (or gain). By changing n_1'' (or $-n_2''$), we have studied the real parts and imaginary parts of the eigenfrequencies. All the results are summarized in Figs. 3(a) and 3(b). When $n_1'' = -n_2'' = 0$, the cavity is a conventional hybrid plasmonic nanocavity. Thus a series of hybrid plasmonic modes have been observed. The field distribution in the transverse plane (x-y plane) is similar to Fig. 1(b). The mode profiles in z direction consist of periodic nodes and the maximal values within every two nodes are quite similar (see examples in top panel of Fig. 3(c)). Thus it is easy to know that these resonances are Fabry-Perot modes with mode numbers $m = 68 - 71$.

With the increase of gain (n_1'' or $-n_2''$), the real and imaginary parts of eigenfrequencies show quite different behaviors from conventional plasmonic nanolasers. As shown in Fig. 3(a), the real parts of frequencies change slightly at the beginning. Once n_1'' is larger than 0.04, two resonant modes approach each other quickly and merge. Meanwhile, the imaginary parts keep as constants and finally bifurcate. All these behaviors are very similar to the theoretical model in Figs. 2(a) and 2(b), clearly demonstrating the broken PT symmetry in our hybrid plasmonic nanocavity.

As the resonant frequencies of two nearby modes merge to the same frequencies, the mode spacing of final lasing modes are thus doubled after the PT symmetry breaking[29,30]. This is one difference between PT symmetric Fabry-Perot lasers and microdisks lasers. In the latter case, the modes with the same Azimuthal numbers couple each other. Compared with the doubled mode spacing, the field profiles of lasing and absorption modes are more interesting. In conventional PT symmetric lasers, the lasing and absorption modes are simply considered to be localized within gain and loss regions. In our hybrid plasmonic nanocavity, the mode profiles are more complicated[30].

In Fabry-Perot cavity, the mode at resonance ω can be expressed as

$$\nabla^2\psi(x) + n_i^2(\frac{\omega}{c})^2\psi(x) = 0, \quad (5)$$

where $\phi(x)$ is the field distribution, $n_i = n_L, n_R$ at left and right regions, and c is the speed of light in vacuum. Then the mode profile within the gain region can be written as

$$\psi(x) = a_+ e^{in_L kx} + a_- e^{-in_L k(x-L/2)}. \quad (6)$$

Here k is ω/c, a_+, a_- are the amplitudes of forward and backward propagating waves, respectively.[30]. At lasing threshold, the usual round trip phase and amplitude condition for FP cavity is $r_1 r_2 exp(in_L L) = 1$, where r_1 and r_2 are the reflectivity at the left end-facet and gain-loss interface. Then the ratio between forward and backward propagating waves is

$$|\frac{a_+}{a_-}| = |r_1|e^{n_L kL/2} = \sqrt{|\frac{r_1}{r_2}|}. \quad (7)$$

In the case of hybrid plasmonic waveguide[11], the effective refractive indices of plasmonic mode in gain and loss regions are 2.3+0.047068i and 2.3-0.052053i, respectively. We can see that the refractive index difference between hybrid waveguide and air is much larger than the one between gain and loss regions. Following the Fresnel equations, it is easy to get the result $r_1 \gg r_2$. Consequently, the lasing mode in gain region is dominated by the right-propagating waves. From Eq. (6), we know that the electric field is amplified before it reaches the gain-loss interface. Then the amplitude of electric field reaches maximum at the gain-loss interface. Following Eqs. (6) and (7), similar phenomenon holds true for the absorption mode too. Thus both of them can be considered as surface modes after PT symmetry breaking.

Such kind of surface modes have been observed in our numerical calculations. As show in the bottom panel of Fig. 3(c), we can see that the electric fields of both lasing mode

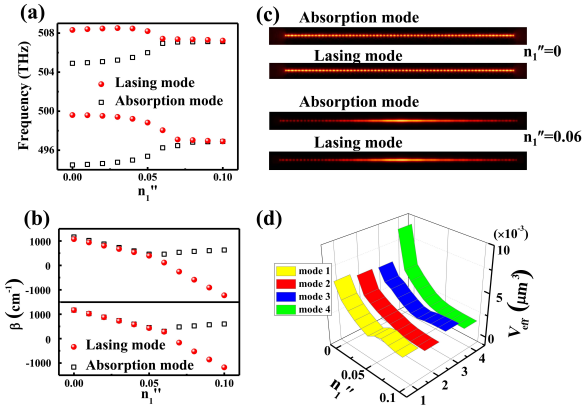

Fig. 4 Quasi-PT symmetry breaking in hybrid plasmonic nanocavity. The same as Figure 3 except n_2" is fixed at -0.05.

and absorption modes are mainly confined around the gain-loss interface. The intensity of resonant mode increases exponentially from left end-facet to the gain-loss interface and then reduces exponentially. Taking account of the two-dimensional mode confinement (Fig. 1(b)), we thus know that full three-dimensional light confinement has been obtained by applying the PT symmetry. Such kind of thee-dimensional light confinement is important for V_{eff}. Following the definition of effective mode volume ($\int\int\int W(r)d^3r/max(W(r))$), it is easy to know that V_{eff} is inversely proportional to the maxima value of field. Therefore, the V_{eff} in PT symmetric nanocavities can be further improved. The results are plotted in Fig. 3(d). With the increase of n_1'', V_{eff} reduces very quickly. When n_1'' is larger than 0.06, V_{eff} is leveling out at around 0.00169 μm^3, which is much smaller than the one of conventional hybrid plasmonic mode. Therefore, applying PT symmetry to hybrid plasmonic nanolasers can effectively improve the effective mode volume and the corresponding light matter interaction within nanocavities.

As shown in Figs. 2(c) and 2(d), similar PT-symmetric phenomena can also be observed in systems with fixed loss. Thus it is also interesting to explore the behaviors in quasi-PT symmetric systems. One example is depicted in Fig. 4. Similar to Fig.3, four Fabry-Perot modes with $m = 68-71$ have been considered. With the increase of n_1'', their real parts also slightly approach each other and merge quickly at $n_1'' \sim 0.06$. At the same time, the imaginary parts of all resonance approach to zero first and then bifurcate. One resonance of each mode pair turns to be lasing mode and the other one transits to lossy mode simultaneously. Figures 4(c) illustrates the corresponding field distributions at $n_1'' = 0$ (top panel) and $n_1'' = 0.06$ (bottom panel), respectively. After the breaking of PT symmetry, we can see that both lasing mode and absorption mode are confined well at the gain-loss interfaces. Consequently, the effective mode volume can also been significantly improved (see Fig. 4(d)). It's also worth noting that the refractive index of the active medium (CdS for our case) will be modified when gain is applied to CdS nanowire in our model. Thus it is essential to investigate the robustness of the PT-symmetric behaviors with modal dispersion induced by CdS. We calculated the PT-symmetry breaking phase when the real part of the refractive index of CdS changes from 2.5 at $n_1'' = 0$ to 2.56 at $n_1'' = 0.1$. The PT-symmetry breaking and mode bifurcation still occur at $n_1'' = 0.06$, clearly demonstrating the robust phenomenon of modal localization in the case of PT-symmetric system with material dispersion.

In conclusion, we have studied the light confinements within the hybrid plasmonic nanocavity with PT symmetry. In additional to the two-dimensional light confinement in the transverse plane, the light is mostly localized around the gain-loss interface along the third dimension by breaking the PT symmetry or quasi-PT symmetry. Such kinds of surface modes have provided a way to improve the light confinement in all three dimensions. Consequently, the V_{eff} after PT symmetry breaking can be as small as 0.00169 μm^3, which is much smaller than conventional hybrid plasmonic nanocavity. We note that V_{eff} can be further improved if the periodic structures and PT symmetry are applied simultaneously onto the hybrid plasmonic nanolasers. We believe that our research will be interesting for the study of light-matter interaction in nanocavities.

Method

Numerical settings. In this letter, finite element method (FEM, Comsol Multiphysics 4.3a) is employed to calculate the eigenfrequency of the resonant modes in the hybrid plasmonic nanocavity. 3D eigenfrequency study from Radio Frequency module is utilized to search the eigenvalues of the cavity. The complex refractive index is n=n + ik with k $>$ 0 for gain and k $<$ 0 for loss. The simulation region is terminated with Perfectly Matched Layer (PML) and Scattering Boundary Condition to absorb the scattering energy. Eigenvalue solver is used to find the complex resonance frequency $f = f_{real} + if_{imag}$. The effective mode volume can be expressed as

$$V_{eff} = \frac{\int\int\int W(r)d^3r}{max(W(r))}. \quad (8)$$

where W(r) is energy density of the cavity and takes the form

$$W(r) = \frac{1}{2}(\mu_0|H(r)|^2 + \frac{d(\varepsilon(r)\omega)}{d\omega}|E(r)|^2) \quad (9)$$

Acknowledgement

This work is supported by NSFC11204055, NSFC61222507, NSFC11374078, NCET-11-0809, KQCX2012080709143322, KQCX20130627094615410, JCYJ20140417172417110, and JCYJ20140417172417096.

References

1 Y. Akahane, T. Asano, and B. S. Song, *Nature*, **2003**, *425*, 6961.
2 A. Shacham, K. Bergman, L. P. Carloni, *IEEE Trans. on Computer*, **2008**, *57*, 1246.
3 R. M. Ma et al., *Nanotechnology*, **2007**, *18* 205605.
4 W. L. Barnes, A. Dereux, and T. W. Ebbesen, *Nature*, **2003**, **424**, 824.
5 Q. H. Song, H. Cao, S. T. Ho, and G. S. Solomon, *Appl. Phys. Lett.* **2009**, *94*, 061109.
6 M. H. Huang et al., *Science*, **2001**, *292*, 1897.
7 D. J. Bergman, and M. I. Stockman, *Phys. Rev. Lett.*, **2003**, *90*, 027402.
8 M. A. Noginov et al., *Nature*, **2003**, *460*, 7259.
9 W. Zhou et al., *Nat. Nanotech.*, **2013**, *8*, 506.
10 C. Zhang et al., *Nano Lett.*, **2015**, *15*, 1382.
11 R. F. Oulton et al., *Nature*, **2009**, *461*, 629.
12 C. Y. Wu et al., *Nano Lett.*, **2011**, *11*, 4256.
13 R. M. Ma, R. F. Oulton, V. J. Sorger, G. Bartal, and X. Zhang, *Nat. Mater.*, **2011**, *10*, 110.
14 J. Li et al., *Nanoscale*, **2013**, *5*, 8494.
15 T. P. H. Sidiropoulos et al., *Nat. Phys.*, **2014**, *10*, 870.
16 J. T. Robinson, C. Manolatou, L. Chen, and M. Lipson, *Phys. Rev. Lett.*, **2005**, *95*, 143901.
17 C. M. Bender, and S. Boettcher,*Phys. Rev. Lett.*, **1998**, *80*, 5243.
18 C. E. Rüter, K. G. Makris, R. El-Ganainy, D. N. Christodoulides, M. Segev, and D. Kip, *Nat. Phys.*, **2010**, *6* 192.
19 Y. D. Chong, L. Ge, and A. D. Stone, *Phys. Rev. Lett.*, **2011**, *106*, 093902.
20 B. Peng et al., *Nat. Phys.*, **2014**, *10*, 394.
21 Z. Lin, H. Ramezani, T. Eichelkraut, T. Kottos, H. Cao, and D. N. Christodoulides, *Phys. Rev. Lett.*, **2011**, *106* 213901.
22 L. Feng, Z. J. Wong, R. M. Ma, Y. Wang, and X. Zhang, *Science*, **2014**, *346*, 972.
23 H. Hodaei, M. A. Miri, M. Heinrich, D. N. Christodoulides, and M. Khajavikhan, *Science*, **2014**, *346*, 975.
24 Q. H. Song, J. K. Li, W. Z. Sun, N. Zhang, S. Liu, M. Li, and S. M. Xiao, *Opt. Express*, **2015**, *23*, 24257.
25 L. GE, and A. D. Stone, *Phys. Rev. Lett.*, **2014**, *4*, 031011.
26 Z. Y. Gu et al., *Sci. Rep.*, **2015**, *5*, 9171.
27 R. EI-Ganainy, M. Khajavikhan, and L. Ge, *Phys. Rev. A*, **2014**, *90*, 013802.
28 S. Longhi, *Phys. Rev. A*, **2010**, *82*, 031801.
29 Z. Y. Gu et al., Arxiv:1505.03937 (2015).
30 L. Ge, Y. D. Chong, S. Rotter, and A. D. Stone, *Phys. Rev. A*, **2011**, *84*, 023820.